Improvement of Oxygen Barrier of Oriented Polypropylene Films Coated by Gravure Ink-Containing Nanoclays

Seok-Hoon Park,[1] Seong Jin Kim,[1] Hyun Soo Lee,[2] Jae Hoon Choi,[2] Chang Myeong Jeong,[2] Myoung Hwan Sung,[2] Dong Hyun Kim,[3] Hyun Jin Park[1,4]

[1]*College of Life Sciences and Biotechnology, Korea University, 5-Ka, Anam-Dong, Sungbuk-Ku, Seoul 136-701, Republic of Korea*
[2]*Research Development Department, Lotte Aluminum, 1005 Doksan-Dong, Geumcheon-Gu, Seoul 153-010, Republic of Korea*
[3]*Korea Institute of Industrial Technology, Bucheon-Si, Gyeonggi-Do 421-742, Republic of Korea*
[4]*Department of Packaging Science, Clemson University, Clemson, South Carolina 29634-0320*

Received 30 November 2009; accepted 26 September 2010
DOI 10.1002/app.33457
Published online 8 March 2011 in Wiley Online Library (wileyonlinelibrary.com).

ABSTRACT: The feasibility of a gravure ink-containing nanoclays as an alternative oxygen (O_2) barrier material to oriented polypropylene (OPP) film was investigated. The gravure ink was effectively dispersed through the clay using an ultrasonic homogenizer. Barrier properties of OPP films coated by the gravure ink-containing nanoclays were evaluated with respect to dispersion time, clay content, and different types of nanoclays (Cloisite Na^+, Cloisite 25A, and Cloisite 30B). Barrier and morphology properties of the OPP films were tested by measuring selected film properties such as O_2 transmission rate (OTR), and water vapor transmission rate, and by field emission scanning electron microscopy, X-ray diffraction (XRD), and transmission electron microscopy (TEM). OTR of control OPP film coated solely with gravure ink was 1653 cm^3 m^{-2} day, while use of OPP films coated by the three different types of gravure ink-containing nanoclays (nanoclay content: 1% w/w) reduced OTR by 12–37%. OTR values measured using the gravure ink-containing modified montmorillonite (Cloisite 25A and Cloisite 30B) were markedly lower than measured by pristine gravure ink-containing unmodified montmorillonite (Cloisite Na^+). On the other hand, no remarkable differences were evident in the water vapor barrier performance of control OPP film and gravure ink-containing nanoclay-coated OPP film. As nanoclay content and dispersion time increased, OTR values of the OPP films coated by gravure ink-containing nanoclays decreased. And the TEM and XRD observation indicated that intercalated and exfoliated types were generated. © 2011 Wiley Periodicals, Inc. J Appl Polym Sci 121: 1788–1795, 2011

Key words: barrier; clay; poly(propylene); (PP); films; coatings

INTRODUCTION

To enhance the unique properties of polyolefin films, many approaches have been tried to prepare polymer/nanoclay composites. These include *in situ* polymerization of ethylene in the presence of layered silicate, solvent blending, and melt compounding.[1–4] Consequent improvements have included increased strength, higher modulus, thermal stability, enhanced barrier properties, and decreased flammability. Hence, to capitalize on the potential offered by nanoparticles in areas such as reinforcement, barrier, and electrical conductivity, higher levels of fully dispersed nanoparticles must be obtained.[5]

Recently, these composites are a class of hybrid materials composed of polymer matrices and nanoclay. Because of their high aspect ratios and high surface area, if clay particles are properly dispersed in the polymer matrix at a loading level of 1–5% (w/w), unique combinations of physical and chemical properties will be obtained, which in turn make these composites attractive for the preparation of films and coatings for a variety of industrial applications.[6,7]

Also, most schemes to improve the gas barrier property of polyolefins involve either addition of higher barrier plastics via a multilayer structure or high barrier surface coatings; however, these approaches are not cost effective.[8,9] Also, excellent barrier properties may be obtained by disposition of aluminum vapor or by plasma-assisted deposition of inorganic layers such as silicon oxide on common polymeric films.[10,11] However, these surface modification processes are technologically sophisticated (e.g., vacuum or plasma) and expensive.

In this research, another approach was that OPP films with barrier properties were printed by gravure ink-containing nanoclays. Additional printing was simple and inexpensive compared with the

Correspondence to: Dr. H. J. Park (hjpark@korea.ac.kr).
Contract grant sponsor: Development of Eco-Packaging Solution Technology; contract grant number: 100031979.

approaches mentioned above. So, usage of gravure ink-containing nanoclays could reduce manufacturing costs.

The nanoclay known as montmorillonite (MMT) consists of platelets. Its structure consists of several stacked layers, with a layer thickness around 0.96 nm and a lateral dimension of 100–200 nm. These layers organize themselves to form stacks with a regular intervening gap, called the interlayer or gallery. The sum of the single layer thickness and the interlayer represents the repeat unit of the multilayer material, called the *d*-spacing or basal spacing (d_{001}), which is calculated from the (001) harmonics obtained from X-ray diffraction (XRD) patterns.[5] The negative charges are generated by isomorphous substitution that occurs in the octahedral sheets, and they are counterbalanced by gallery cations such as Na^+.

Because of the presence of cations adsorbed on the silicate layer, cations inside the gallery can be easily exchanged by other cations. Substitution of Ca^{2+} and Na^+ by organic cations leads to a more organophilic filler than the original hydrophilic clay and facilitates the separation of the clay layers. Alkyl ammonium salts have been used to treat unmodified clay. This process allows resin penetration between the clay layers, producing clay exfoliation.[12,13]

For most purpose, complete exfoliation of the clay platelets, separation of platelets from one another, and dispersed individually in the polymer matrix, is the desired goal of the formation process. However, this ideal morphology is frequently not achieved and varying degrees of dispersion (immiscible, intercalated, miscible, or exfoliated) are more common.[14]

The dispersion of MMT, with its high aspect ratio and extremely high surface-to-volume ratio, represented a significant improvement of the polymer matrix in terms of mechanical properties, function as a gas barrier, and optical properties at low filler content.[12,15–18] The simple mechanism by which an organoclay can improve barrier properties relies on the high aspect ratio of the intercalated clay platelets to impart a tortuous path that retards the transport of diffusing species such as O_2, carbon dioxide, or water vapor to the same degree.[2] To selectively enhance the transport barrier function, the use of different organoclay/polymer nanocomposites has been explored.[19–21]

The main objective of this study was to improve the O_2 barrier properties of OPP films coated by gravure ink-containing nanoclays using an ultrasonic homogenizer for the dispersion of the intercalated platelets, and to determine some selected properties including oxygen transmission rate (OTR), water vapor transmission rate (WVTR), field emission scanning electron microscopy (FESEM), XRD, and transmission electron microscopy (TEM).

MATERIALS AND METHODS

Materials

Two organically-modified MMTs (Cloisite 25A and 30B) with a respective modifier concentration of 95 meq/100 g and 90 meq/100 g, and unmodified MMT (Cloisite Na^+) were supplied by Southern Clay Products (USA). Ink (color: transparency white) and solvent (ingredient: methyl ethyl ketone and ethyl acetate) were supplied by IPC (South Korea). OPP films of 20 μm thickness were supplied by Youl Chon Chemical (South Korea).

Preparation of OPP films coated by gravure ink-containing nanoclay

Ink solution was prepared by mixing ink and solvent in a 1 : 1 (v/v) ratio. This ink solution was fully mixed using a mechanical stirrer prior to the addition of 0–3% by weight ink solution followed by vigorous stirring. These suspensions were fully mixed using a magnetic stirrer and were dispersed using an ultrasonic homogenizer for varying dispersion times (0–60 min). After ultrasonic homogenization, OPP films were individually coated with each suspension using an automatic film applicator (Yasuda, Japan). In the case of Cloisite Na^+, because of a precipitate that formed (Fig. 1), supernatant was used to prepare the uniform coating on OPP films. The coating speed was 300 mm s^{-1} at 60 Hz. The ink/nanoclay-coated OPP films were dried at ambient conditions for 24 h.

OTR

OTR of films was measured using an OX-TRAN® Model 2/61 apparatus (MOCON, USA). OTR represents the ease with which O_2 traverses films when submitted to a gradient in the partial pressure of O_2 across the films. It is expressed as the quantity (Q) of O_2 molecules passing through a film surface area (A) during time (t) at steady state under a partial pressure difference (Δp) in O_2 between the two surfaces of the sample:

$$\mathrm{OTR} = Q/A\ t \cdot \Delta p \tag{1}$$

Testing was performed at 23°C under an RH of 0%. OTR was measured as cm^3 m^{-2}·day. Measurements were taken three times and the average value was calculated. All specimens were conditioned at ambient conditions.

Water vapor transmission rate (WVTR)

WVTR of films was measured by using a PERMATRAN-W® Model 3/61 apparatus (MOCON). The test film was first placed into the six test cells. As

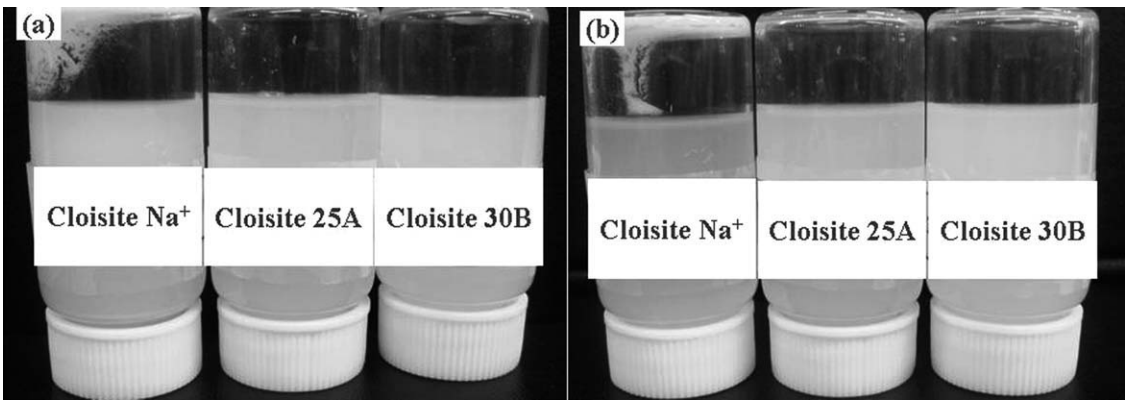

Figure 1 The effect of nanoclay type on precipitation of ink/nanoclay solutions after (a) 1 h and (b) 24 h.

the water vapor diffused through the test film, it was carried by carrier gas (N_2) to the detector, and WVTR was continuously recorded. Permatran response was calibrated using a reference film provided by the manufacturer. The test was done in triplicate and average mean value was used. Testing was performed at 38°C under a relative humidity of 100%. WVTR was obtained in g m^{-2}·day. All specimens were conditioned at ambient conditions.

Haze

Haze is the scattering of light as it passes through a transparent material, resulting in poor visibility and/or glare. Transmittance measures the amount of light that passes through a sample. Haze and transmission measurements can be useful in product development, process development, and end-use performance testing. Film haze was measured using a Model NDH5000 haze meter (Nippon Denshoku Industries, Japan). The double-beam measurement system utilized a 150-mm integrating sphere with a compensating aperture, applied barium sulfate, and a hatch type trap. The light source was a white light-emitting diode. Triplicate measurements were performed with individually prepared film samples and the average value was calculated.

Field emission scanning electron microscopy (FESEM)

Film surface morphology was measured by Field Emission Scanning Electron Microscopy (FESEM) using a MIRA II LM apparatus (Tescan, Czech Republic) operating at 5.0 kV. Images at 1000× magnification were acquired.

X-ray diffraction (XRD)

Wide-angle XRD patterns of film specimens were recorded using small-angle X-ray scattering (SAXS). The apparatus was equipped with a General Area Detector Diffraction System (GADDS; Bruker AXS, Germany). The area detector operated at a voltage of 40 kV and a current of 45 mA with Cu Kα radiation ($\lambda = 0.15406$ nm). The basal spacing of silicate layer (d_{001}) was calculated using Bragg's eq. (2), allowing calculation of the gap between nanoclay layers:

$$2d \sin\theta = n\lambda \qquad n = 1, \lambda = 1.5406 \text{ Å} \tag{2}$$

Equation (2) can be applied when the XRD angle is small. Parameter definition is as follows: d is the spacing between the diffracting lattice planes, θ is the measured diffraction angle, n is an integer, and λ is the wavelength of the X-ray radiation used.

Transmission electron microscopy (TEM)

For TEM observation, 70-nm sections of the samples were prepared by cutting the sample at room temperature using ultramicrotome at a cutting speed of 0.6 mm s^{-1}. The sections were collected in a water-filled trough and placed on 200-mesh copper grids, and were cut perpendicular to the surface of the film. The TEM images were taken with a Philips Tecnai 12 transmission electron microscope at an accelerating voltage of 120.0 kV and the HRTEM images and SAED patterns were taken with a FEI Tecnai 20 transmission electron microscope equipped with a TVIPS CCD camera at an accelerating voltage of 200.0 kV.

Statistical analysis

The measurement of OTR, WVTR, and Haze were measured using individually-coated films in triplicate, as the replicated experimental units. The significance of each mean property value was determined

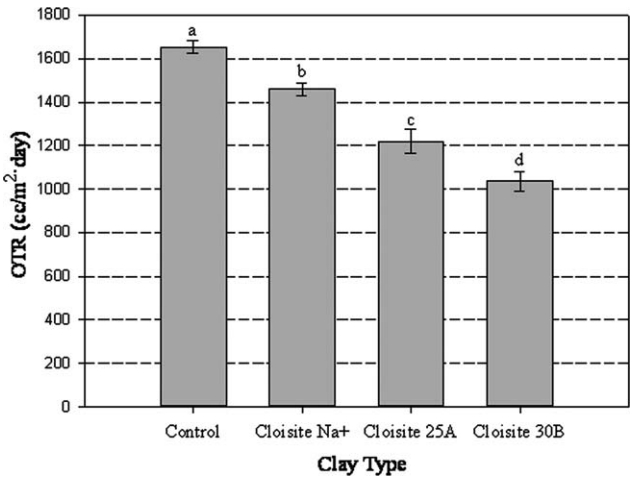

Figure 2 OTR of OPP films coated by gravure ink-containing three different types of nanoclays. The control was OPP film coated by only the gravure ink solution.

($P < 0.05$) with Duncan's multiple range tests in the SAS software. Each value in the figure is the mean of three replicates with the standard deviation. Any two means in the same figure followed by the same letter are not significantly ($P > 0.05$) different by Duncan's multiple range test.

RESULTS AND DISCUSSION

Effect of nanoclay type on OTR

The OTRs of control OPP films and OPP films coated by gravure ink-containing nanoclays are shown in Figure 2. The OTR value of control OPP films was 1653 cm^3 m^{-2}·day, and the OTR values of OPP films coated by gravure ink-containing nanoclays were lower: 1460, 1219, and 1037 cm^3 m^{-2}·day for Cloisite Na^+, Cloisite 25A, and Cloisite 30B, respectively. Particularly, the OTR of OPP films coated by the gravure ink-containing nanoclay decreased dramatically depending on the types of nanoclays used. The OTR values of OPP films coated by gravure ink-containing modified MMT (Cloisite 25A and 30B) were much lower than that of OPP films coated by gravure ink-containing unmodified MMT (Cloisite Na^+). This result indicates that modified MMT is more effectively dispersed in ink solutions than pristine MMT. Between the two modified MMTs, Cloisite 30B was more effective in reducing OTR than Cloisite 25A, indicating that Cloisite 30B is more ink-compatible. The increase in O_2 barrier property of OPP films coated by gravure ink-containing nanoclays is attributed to the tortuous path for O_2 diffusion due to more compact arrangement of impermeable nanoclays layers on OPP films, which consequently increases the effective diffusion path length.

In case of polymer/nanoclay composites, addition of nanoclay to a pure polymer film improves barrier properties,[22,23] due to the combination of two phenomena: decreased area available for diffusion due to the replacement of preamble polymer by the impermeable nanoclays, and the increased distance a solute must travel to cross the film as it follows a tortuous path around the impermeable nanoclays.[24,25]

Effect of nanoclay type on WVTR

Figure 3 shows the WVTR of control OPP films and OPP films coated by gravure ink-containing nanoclays. Similar values were observed for all samples, indicating that gravure ink-containing nanoclays are ineffective in reducing the water vapor barrier.

On the other hand, in case of polymer/nanoclay composites, WVTR can be significantly improved by incorporation of micro/nanoclay in the film matrix.[26] Also, WVTR of nanocomposite films can change significantly depending on the type of nanoclays used. WVTR increases for nanocomposite films compounded with modified nanoclays, while the value decreases slightly for unmodified nanoclay.[27]

Effect of nanoclay content on OTR

The effect of nanoclay content on OTR of the OPP films coated by gravure ink-containing Cloisite 30B is shown in Figure 4. To test the effect of nanoclay content, OPP films coated by gravure ink-containing Cloisite 30B were prepared by varying the nanoclay content from 0 to 3% (w/w). The OTR value of control OPP films (nanoclay content of 0%) was 1653 cm^3 m^{-2}·day, and the OTR values of OPP films coated by gravure ink-containing nanoclay were lower: 1037, 961, and 861 cm^3 m^{-2}·day for 1, 2, and

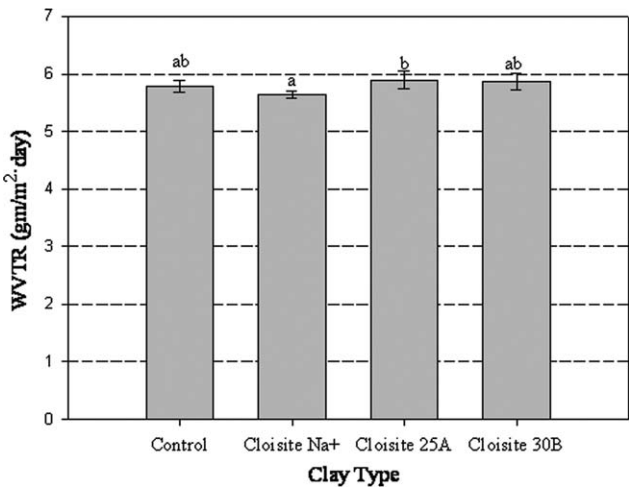

Figure 3 WVTR of OPP films coated by gravure ink-containing three different types of nanoclays. The control was OPP film coated by only the gravure ink solution.

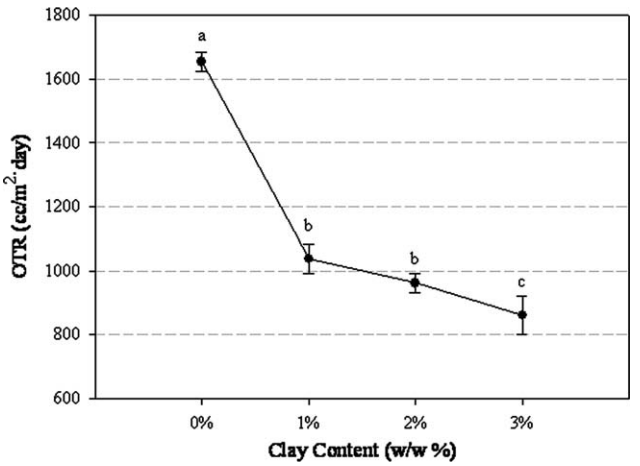

Figure 4 The effect of nanoclay content on OTR of OPP films coated by gravure ink-containing Cloisite 30B.

3%, respectively. The OTR values of the OPP films decreased significantly up to nanoclay content of 1%, followed by a slight decrease with further increase up to 3%. Adding higher concentration, like 4% than 3% of Cloisite 30B, gravure ink-containing nanoclay would gel overnight. So the suspension wasn't suited for application. Considering cost and efficiency of commercial production, a nanoclay content of 1% may be both practically suitable and economical for use as an O_2 barrier.

In case of polymer/nanoclay composites, many reports have provided evidence that the barrier properties of polymer/nanoclay composite films decrease significantly with increases in clay content.[25,27,28]

Effect of dispersion time on OTR

Figure 5 summarizes the effect of dispersion time on OTR of OPP films coated by gravure ink-containing Cloisite 30B prepared by varying the dispersion time from 0 to 60 min. The OTR value of OPP films prepared by dispersion time of 0 min was 1610 cm^3 m^{-2}·day, and the OTR values of OPP films coated by gravure ink-containing nanoclays were lower: 1037, 995, and 955 cm^3 m^{-2}·day for 20, 40, and 60 min, respectively. The OTR of the OPP films decreased dramatically at dispersion time of 20 min, followed by a slight decrease with further increase in dispersion time up to 60 min. Considering cost and efficiency of commercial production, the use of a 20-min dispersion time is both functionally sufficient and economically prudent.

In case of polymer/nanoclay composites, changing the shear rate did not significantly influence O_2 barrier property. But, ultrasonicated films showed improved barrier property against O_2. From this result, it can be suggested that increased degree of exfoliation of nanoclay in film samples leads to improved barrier property against O_2 permeation.[28] And, the degree of dispersion, are improved when the mixing time increases, at least up to 20 min.[29]

Field emission scanning electron microscopy (FESEM)

FESEM images of the OPP films coated by gravure ink-containing three different types of nanoclays are shown in Figure 6. The images of unmodified MMT (Cloisite Na^+) on the OPP films coated by gravure ink-containing nanoclays were large as compared to modified MMT (Cloisite 25A and 30B), which was evidence of the enhanced dispersion of modified MMT and ink solutions achieved by the ultrasonic homogenization.

In case of polymer/nanoclay composites, the dispersed phase in nanocomposite membranes became more spherical in shape and the size of the domains decreased.[2] And with the addition of modified nanoclay, the aggregates were small, confirming that better dispersion of modified nanoclay and PP matrix was achieved.[30]

Haze property

The haze of OPP films coated by the three different types of gravure ink-containing nanoclays was higher than that of the control OPP films (Fig. 7), which is consistent with observations of hindered light passage by impermeable nanoclays. Furthermore, the haze of the OPP films coated by gravure ink-containing modified MMT (Cloisite 25A and 30B) were much higher than that of OPP films coated by gravure ink-containing unmodified MMT (Cloisite Na^+), due to more compact arrangement of impermeable nanoclays.

In case of polymer/nanoclay composites, the optical property of a well-developed nanocomposite

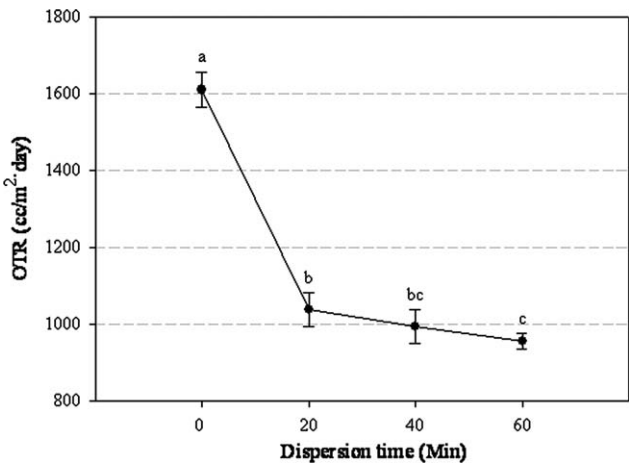

Figure 5 The effect of dispersion time on OTR of OPP films coated by gravure ink-containing Cloisite 30B.

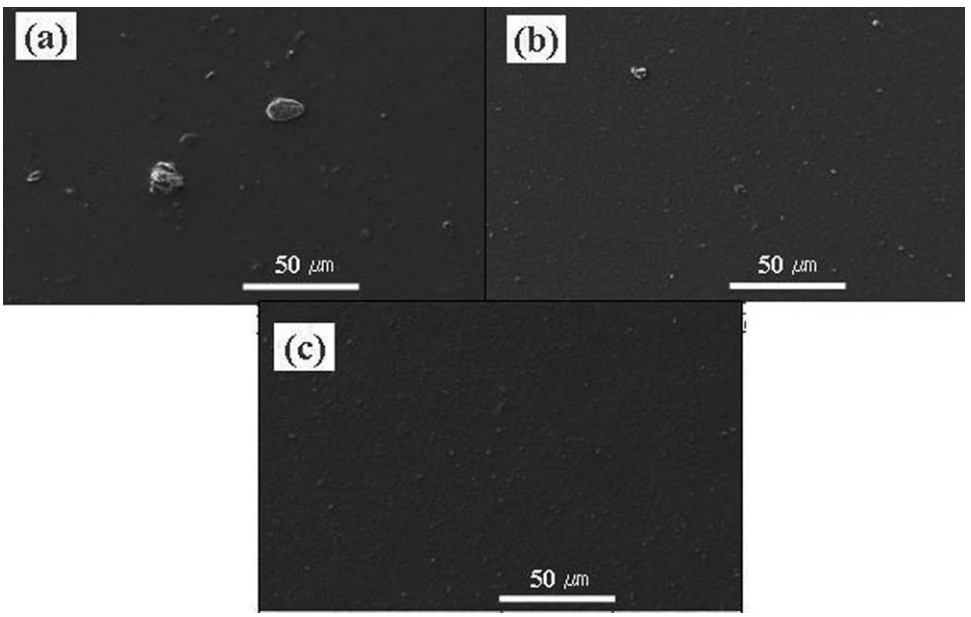

Figure 6 FESEM micrograph of OPP films coated by gravure ink-containing three different types of nanoclays: (a) Cloisite Na^+; (b) Cloisite 25A; (c) Cloisite 30B.

film is generally not significantly changed when clay platelets with a thickness of about 1 nm are well dispersed through the polymer matrix, since the particle's diameter is less than the wavelength of visible light, and so the passage of light is unhindered.[31] However, the large decrease in the transmittance of the composite films indirectly indicates an incomplete dispersion of the clays in the polymer matrix. Also, the transmittance of the composite films decreased linearly with increases in clay content.[27]

X-ray diffraction (XRD)

The XRD patterns of Cloisite Na^+, 30B, and 25A revealed the diffraction peaks at $2\theta = 7.41°$, $2\theta = 4.89°$ and $2\theta = 4.04°$, respectively, (Fig. 8), suggesting a layer distance of 1.19, 1.81, and 2.20 nm, respectively. The main peak of the nanoclays was shifted to a lower angle, corresponding to an increase in *d*-spacing to 6.09 nm for the OPP films incorporating the three types of gravure ink-containing nanoclays. The higher basal spacings of these OPP films, as compared to nanoclays, were attributable to the effective dispersion through the use of ultrasonic homogenization. Careful inspection of the XRD patterns of the OPP films using gravure ink-containing nanoclays indicates that the nanoclays can form an intercalated or exfoliated nanostructure.

This is similar to polymer/nanoclay composites, in which the specific peak of nanoclays moved to lower angle, corresponding to an increase in *d*-spacing for polymer/clay composites. The higher basal spacing of clays in the polymer/clay composites, are due to the intercalation of polymer chains inside the clay layers. Also, the mixed state of intercalated or exfoliated structure could be observed in various weight compositions with modified nanoclay.[27,32]

Transmission electron microscopy (TEM)

Along with the XRD, the TEM is one of the main tools used for determination of the dispersion of the clay nanoparticles.[31] The TEM images of OPP films coated by gravure ink-containing Cloisite 30B were shown in Figure 9(a,b). Cloisite 30B layers were well-ordered and dispersed using an ultrasonic homogenizer at dispersion time of 20 min in the gravure ink matrix. It was confirmed that the gap between Cloitsite 30B layers were expanded and

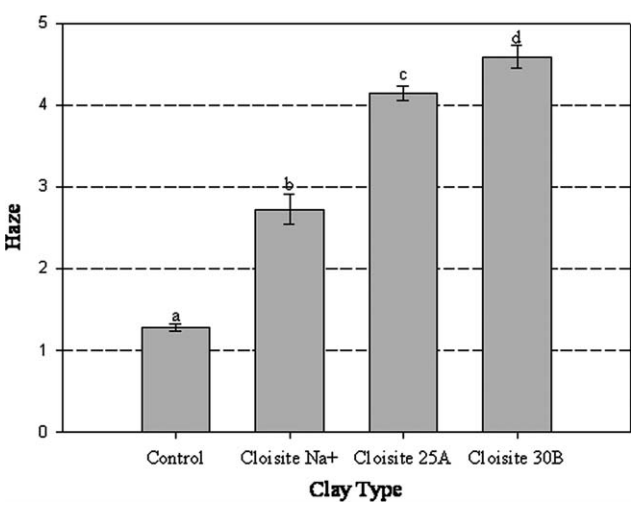

Figure 7 Haze property of OPP films coated by three different types of gravure ink-containing nanoclays.

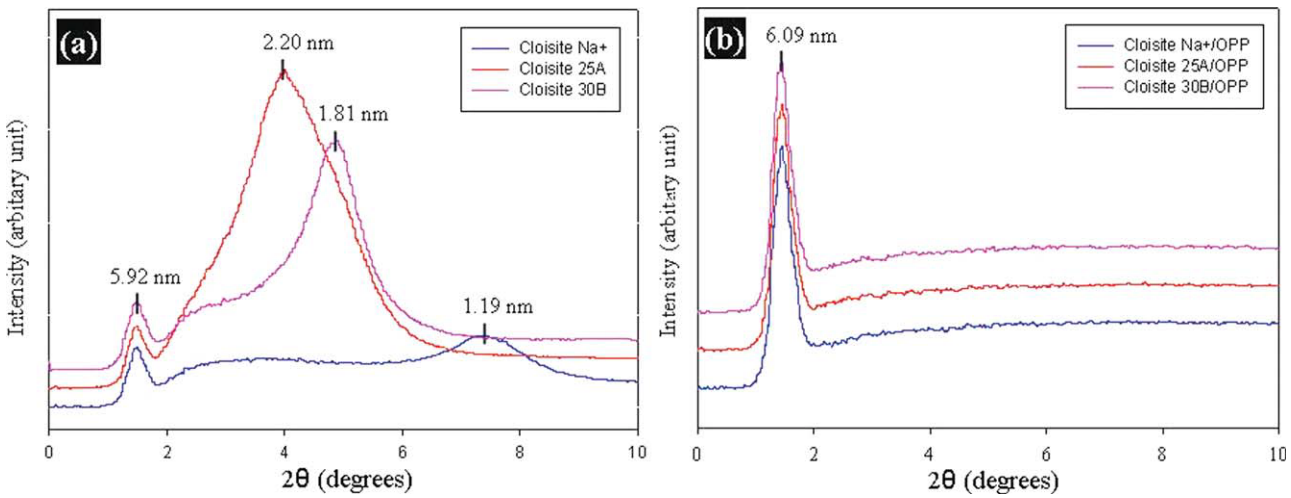

Figure 8 XRD patterns of (a) three different types of nanoclays and (b) OPP films coated by gravure ink-containing three different types of nanoclays. [Color figure can be viewed in the online issue, which is available at wileyonlinelibrary.com.]

that the gravure ink matrices were mainly intercalated and exfoliated into the layers of Cloisite 30B. Therefore, TEM images were consistent with the results of XRD. The results gathered by XRD and TEM observations confirm that the majority of clay particles are in an exfoliated state.

This is similar to polymer/nanoclay composites, it is clearly illustrated that the nanoclay keeps intercalated and exfoliated structure at lower nanoclay content.[33] Also, the TEM images of ultrasonicated polymer/nanoclay composite film were well-ordered and dispersed in the polymer matrix compared with TEM images for nonultrasonicated samples.[28]

CONCLUSIONS

Presently, gravure ink-containing nanoclays could be effectively dispersed by ultrasonic homogenization. Use of gravure ink-containing nanoclays significantly improved the O_2 barrier property of OPP films. The O_2 barrier property of OPP films was also improved by the choice of the optimal modified MMT. The modified MMT (Cloisite 30B and Cloisite 25A) showed enhanced O_2 barrier property than unmodified MMT (Cloisite Na^+). This result indicates modified MMT is more effectively dispersed in ink solutions than unmodified MMT. Between the two types of modified MMT, Cloisite 30B was more effective in reducing OTR than Cloisite 25A. Furthermore, the O_2 barrier property of OPP films coated by gravure ink-containing nanoclay increased with both increasing nanoclay content and dispersion time. These results were related to the structure observed by XRD and TEM. TEM images were consistent with the results of XRD, which indicate that intercalated and exfoliated types

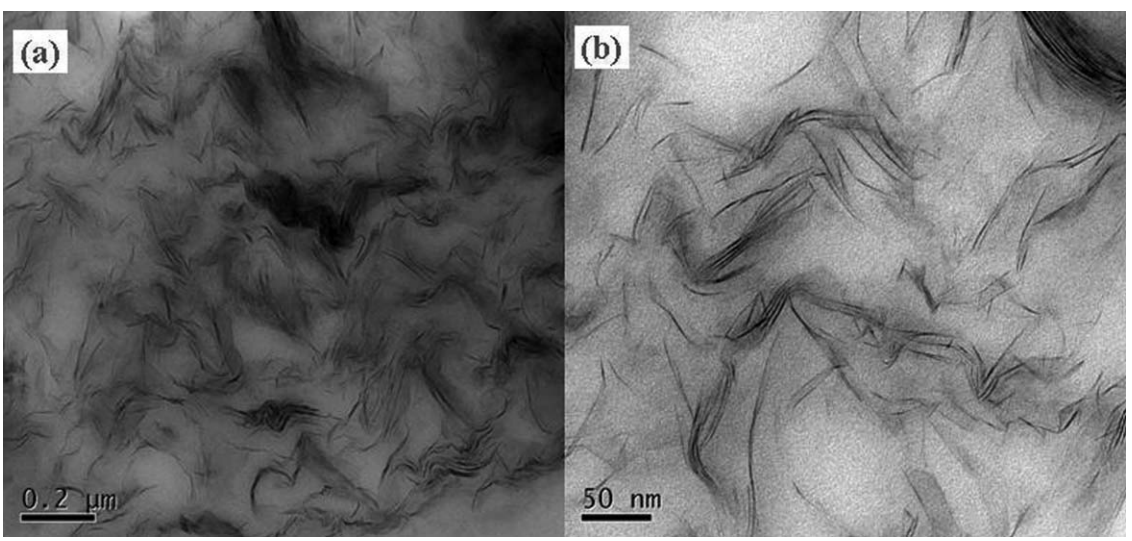

Figure 9 TEM images of OPP films coated by gravure ink-containing Cloisite 30B: (a) low resolution; (b) high resolution.

were generated. Therefore, we conclude that the use of gravure ink-containing nanoclays as barrier materials hold promise as an O_2 barrier. And a nanoclay content of 1% (w/w) and a dispersion time of 20 min achieved the optimum results at the least cost.

References

1. Alexandre, M.; Dubois, P.; Sun, T.; Graces, J. M.; Jerome, R. Polymer 2002, 43, 2123.
2. Song, L.; Hu, Y.; Wang, S.; Chen, Z.; Fan, W. J Mater Chem 2002, 12, 3152.
3. Koo, C. M.; Kim, S. O.; Chung, I. J. Macromolecules 2003, 36, 2748.
4. Bafna, A.; Beaucage, G.; Mirabella, F.; Mehta, S. Polymer 2003, 44, 1103.
5. Anna, J. S.; Mikael, S. H.; Lars, B. Comp Sci Technol 2009, 69, 500.
6. Kim, J. T.; Lee, D. Y.; Oh, T. S.; Lee, D. H. J Appl Polym Sci 2003, 89, 2633.
7. Rhim, J. W.; Hong, S. I.; Park, H.; Perry, K. W. J Agric Food Chem 2006, 54, 5814.
8. Hernandez, R. J.; Selke, S. E. M.; Culter, J. D. Plastic Packaging. Hanser Gardners Publications, 2000; p 313.
9. Masoud, F.; Susan, D.; Zahra, S.; Mohsen, N. J Membr Sci 2006, 282, 142.
10. Amberg-Schwab, S.; Hoffmann, M.; Bader, H.; Gessler, M. J Sol Gel Sci Tech 1998, 13, 141.
11. Inagaki, N.; Tasaka, S.; Nakajima, T. J Appl Polym Sci 2000, 78, 2389.
12. Alexandre, M.; Dubois, P. Mater Sci Eng 2000, 28, 1.
13. Veronic, L.; Bernard, R.; Pierre, B. Prog Org Coat 2008, 62, 400.
14. Paul, D. R.; Robeson, L. M. Polymer 2008, 49, 3187.
15. Brody, A. Food Technol 2003, 61, 80.
16. Giannelis, E. P. Adv Mater 1996, 8, 29.
17. Pandey, J. K.; Kumar, A. P.; Misra, M.; Mohanty, A. K.; Drzal, L. T.; Singh, R. P. J Nanosci Nanotech 2005, 5, 497.
18. Sinha-Ray, S.; Bousmina, M. Prog Mater Sci 2005, 50, 962.
19. Sinha-Ray, S.; Maiti, P.; Okamoto, M.; Yamada, K.; Ueda, K. Macromolecules 2002, 35, 3104.
20. Ogata, N.; Jimenez, G.; Kawai, H.; Ogihara, T. J Polym Sci 1997, 35, 389.
21. Maiti, P.; Yamada, K.; Okamoto, M.; Ueda, K.; Okamoto, K. Chem Mater 2002, 14, 4654.
22. Lape, N. K.; Nuxoll, E. E.; Cussler, E. L. J Membr Sci 2004, 236, 29.
23. Garcia, A.; Eceolaza, S.; Iriarte, M.; Uriarte, C.; Etxeberria, A. J Membr Sci 2007, 301, 190.
24. Yano, K.; Usuki, A.; Okai, A. J Polym Sci 1997, 35, 2289.
25. Cussler, E. L.; Highes, S. E.; Ward, W. J.; Aris, R. J Membr Sci 1998, 38, 161.
26. Casariego, A.; Souza, B. W. S.; Cerqueira, M. A.; Teixeira, J. A.; Cruz, L.; Diaz, R.; Vicente, A. A. Food Hydrocolloids 2009, 23, 1895.
27. Rhim, J. W.; Hong, S. I.; Ha, C. S. LWT 2009, 42, 612.
28. Bae, H. J.; Park, H. J.; Hong, S. I.; Byun, Y. J.; Darby, D. O.; Kimmel, R. M.; Whiteside, W. S. LWT 2009, 42, 1179.
29. Lertwimolnun, W.; Vergnes, B. Polymer 2005, 46, 3462.
30. Sharma, S. K.; Nayak, S. K. Polym Degrad Stab 2009, 94, 132.
31. Xu, Y.; Ren, X.; Hanna, M. A. J Appl Polym Sci 2006, 99, 1684.
32. Quang, T. N.; Donald, G. B. Polymer 2007, 48, 6923.
33. Wang, S. F.; Shen, L.; Tong, Y. J.; Chen, L.; Phang, I. Y.; Lim, P. Q.; Liu, T. X. Polym Dgerad Stabil 2005, 90, 123.